Fall 12-1980

Sound Absorption in N_2-H_2O Gas Mixtures at Elevated Temperatures

Roger W. Meredith
Old Dominion University

SOUND ABSORPTION IN N_2-H_2O GAS MIXTURES AT ELEVATED TEMPERATURES

by
Roger William Meredith
B.S. February 1978, University of Southern Mississippi

A Thesis Submitted to the Faculty of
Old Dominion University in Partial Fulfillment of the
Requirements for the Degree of

MASTER OF SCIENCE

PHYSICS

OLD DOMINION UNIVERSITY
DECEMBER 1980

Approved by:

Dr. A.J. Zuckerwar (Advisor)

A. J. Griffin

Gary E. Copeland

Jacob Becher

James L. Cox, Jr.

ABSTRACT

SOUND ABSORPTION IN N_2-H_2O GAS MIXTURES AT ELEVATED TEMPERATURES

Roger W. Meredith
OLD DOMINION UNIVERSITY, 1980
Thesis Advisor: Dr. A. J. Zuckerwar

Sound absorption measurements were conducted in N_2-H_2O gas mixtures at 297, 343, and 387 Kelvin to determine the location of the vibrational relaxation peak of nitrogen on the frequency/pressure, (f/P), axis as a function of humidity and temperature. At low humidities the best fit of the data is to a linear relationship between $(f/P)_{max}$ and humidity (h) yields a slope of 1.84×10^4 Hz/atm mole fraction at all three temperatures. The slope is the same as that reported by Zuckerwar and Griffin (2.00×10^4 Hz/atm mole fraction) but is lower than the value (2.6×10^4 Hz/atm mole fraction) reported by Chang, Shields, and Bass at higher humidities. These sets of data are shown to be mutually consistent by means of a model in which vibration-vibration transfer is assumed to provide the dominant relaxation path. The results of this work indicate that the relationship between $(f/P)_{max}$ and h written into ANSI Standard S1.26/ASA21-1978 contains an excessively large slope, does not account for the observed transition between low-humidity and high-humidity slopes, and specifies an erroneous temperature dependence.

ACKNOWLEDGEMENTS

The author is much indebted to Dr. Allan Zuckerwar for his invaluable guidance and motivation. The author also wishes to thank Dr. G.E. Copeland and W.A. Griffin for their support and encouragement during the course of this investigation. This work was supported by the National Aeronautics and Space Administration under Grant NSG 1324.

TABLE OF CONTENTS

LIST OF TABLES

LIST OF FIGURES

LIST OF SYMBOLS

μ	sound absorption (neper/wavelength) 1 db = (20 Log_{10} exp) neper
Sx	chart recorder speed (mm/sec)
Sy	potentiometer range/chart width (db/mm)
θ	free decay angle (degrees)
Θ	characteristic temperature (degrees $^{\circ}K$)
f	axial mode frequency (Hz)
Δ	damping half-width associated with wall losses
R	tube radius (cm)
L	tube length (cm)
γ	specific heat ratio
κ	thermal conductivity (cal sec^{-1} cm^{-1} $^{\circ}\text{K}^{-1}$)
η	viscosity (gm sec^{-1} cm^{-1})
ρ	density (gm/cm^3)
Cp	specific heat at constant pressure (cal $\text{gm}^{-1}{}^{\circ}\text{K}^{-1}$)
h	mole fraction water vapor (humidity)
T	temperature ($^{\circ}K$)
S(h)	related to slope, $(f/P)_{max}/h$, via Eq. 14
S1	low humidity approximation to S(h)
S2	high humidity approximation to S(h)

$\bar{\tau}$ mean free time between molecular collisions (sec)

τ molecular vibrational relaxation time (sec)

Na Avagadro's Number

P pressure (atm)

D molecular diameter (m)

M molecular weight (kg/mole)

k Boltzman's Constant (Eq.6)

k probability for deexcitation per molecule per second (Eq.5)

$(f/P)_{max}$ location on the (f/P) axis of maximum absorption due to molecular vibrational relaxation (Hz/atm)

INTRODUCTION

In the last decade experimental studies have demonstrated that nitrogen plays a significant role in sound absorption in the Earth's atmosphere. It is known that the principle mechanism of atmospheric absorption, below 1 kHz, is the vibrational relaxation of the nitrogen molecules in the air.

Recent studies by Zuckerwar and Griffin (Ref.2) have determined the location of the nitrogen vibrational relaxation peak, $(f/P)_{max}$, on the frequency/pressure, (f/P), axis as a function of humidity at room temperature. Their results indicate that the relationship between $(f/P)_{max}$ and h, the mole fraction of water vapor, used in American National Standard Institute (ANSI) Standard S1.26/ASA23-1978 overestimates the shift in $(f/P)_{max}$ by 35-75%, depending on the humidity. They report a linear relationship with an intercept of 0.013 Hz/atm and a slope of 2.00×10^4 Hz/atm mole fraction. Additionally they propose a model in which vibration-vibration transfer is assumed to provide the dominant relaxation path rather than the direct vibration-translation transfer previously favored by other investigators. The present study was motivated by the need to determine the location of the

vibrational relaxation peak of nitrogen as function of humidity and temperature. Acoustical absorption measurements are made in temperature and humidity ranges formerly inaccessible with better accuracy obtained at higher temperatures due to the higher vibrational peak height. These results are compared with that predicted by both the ANSI Standard and the proposed vibration-vibration model.

I. APPARATUS AND EXPERIMENTAL PROCEDURE

Sound absorption is measured by exciting a standing acoustic pressure wave in the test gas, removing the excitation, and recording the natural logarithm of the free decay. The test gas used is a predetermined mixture of nitrogen and water vapor. The humidity of the test gas is determined from a dew point temperature measurement using a hygrometer and converted to water concentration by existing tables. A comprehensive description of the resonant tube, experimental procedure, and data reduction technique, is given in Ref.(3), and only modifications used in this study are discussed. Table I lists the important specifications of the resonant tube used in this experiment.

The acoustical excitation system remains unchanged. For convenience, the second excitation method, employing a rigid piston, is used for static pressures up to 10 atms. The acoustic detector, a PCB high sensitivity quartz microphone, is mounted in a water jacket for cooling the microphone during operation at elevated temperatures. The background broadband noise from the microphone is found to increase proportionally with temperature. Although cooling the microphone does not reduce the background noise, the decay records are not seriously affected. The increased

TABLE I. RESONANT TUBE SPECIFICATIONS

Frequency Range	10-2500	Hz
Pressure Range	1-100	atm
Humidity Range (at 297 °K)	0-2.7	mole %
Temperature Range@	297-387	°K
Length	18.288	m
Bore Diameter	0.152	m
Wall Thickness	0.0254	m

@ Presently being modified to extend the lower temperature range to 273 Kelvin.

noise level is thought to be increased thermal noise of the gas.

The gas handling system remains the same with slight modifications in making ancillary measurements. The test gas static pressure is measured before and after each set of acoustical decay measurements. The temperature of the gas is measured before, during, and after each set of acoustical measurements. The dew point is measured either immediately before or immediately after the acoustical measurements and in some cases both. The gas temperature and/or the pressure is adjusted as many times as needed to obtain acoustical measurements over the desired ranges of these parameters.

The dew point was found to vary with both temperature and pressure. For each gas mixture the dew point increased slightly as the temperature increased. This is due to water adsorbed into the tube walls during the initial charging process, vaporizing as the tube temperature increases. Further, dew point measurements made after the gas had cooled back to room temperature are consistently higher than measurements made before the temperature is cycled. A pressure dependence with humidity, similar to that described in Ref.(2), was observed but not studied. As expected from the Ideal Gas Law, the pressure increased proportionally to the ratio of the final and initial temperature, similarly the sound velocity of the gas increased with the square root of the temperature.

Sound absorption measurements at elevated temperatures proved more difficult than room temperature measurements only at low static pressures (1 atm) where low acoustical excitation and a higher microphone noise level combined to give the poorest decay records and consequently, the greatest data scatter. The Alnor temperature controllers maintained the tube section to within ± 1.5 Celsius of the set temperature so that the tube's temperature gradient did not exceed ± 3 Celsius.

II. THE FREE DECAY RECORD

The nature of the free decay record is discussed thoroughly in Ref.(3). The total sound absorption inside the resonant tube can be calculated from the slope of the decay line using the free decay formula:

$$\mu = \frac{Sx\ Sy\ \tan\Theta}{(20\ \mathrm{Log}_{10}\ \exp)\ f} \qquad (1)$$

where:

μ = sound absorption (neper/wavelength)
Sx = chart speed (mm/sec)
Sy = logarithmic potentiometer range/ chart width (db/mm)
Θ = free decay angle
f = axial mode frequency (Hz)

The free decay angle is measured using an 8.0 inch protractor, with scale markings in 0.5 degree intervals, under an Ednalite Macroscope (magnification 2). Independent measurements using a vernier protractor with 0.1 degree scale markings showed no significant statistical difference in the angle measurement. Similarly, another independent measurement using vernier calipers to measure the length of the decay line, from which the angle is computed showed no significant difference. The error of the angle measurement is estimated at $\pm$ 0.13 degree, or about 0.3% for a slope of 45 degrees.

III. BACKGROUND LOSSES

The total sound absorption inside the resonant tube is due to both molecular relaxation and background losses. The background damping consists of four main contributions. They are thermal and viscous volume, radiation, wall, and apparatus losses. Thermal and viscous volume losses are neglible over the range of frequencies and pressures used in this study (Ref.1) and are not considered. Radiation losses through the endplates and walls of the tube have been shown (Ref.3) to be negligible. The background damping is thus taken to consist entirely of wall and apparatus losses.

The wall losses are computed according to the Kirchhoff Formula (Ref.3) where the damping is in terms of the resonant half width, Δ, and is given by:

$$\Delta = \left[\frac{1}{R} + (\gamma - 1)\left(\frac{\kappa}{\eta C_p}\right)^{1/2}\left(\frac{1}{R} + \frac{2}{L}\right)\right]\left(\frac{f\eta}{\pi\rho}\right)^{1/2} \qquad (2)$$

where

R = tube radius (cm)
L = tube length (cm)
γ = specific heat ratio
κ = thermal conductivity (cal sec^{-1} cm^{-1} $^{\circ}K^{-1}$)
η = viscosity (g sec^{-1} cm^{-1})
C_p = specific heat at constant pressure (cal g^{-1} $^{\circ}K^{-1}$)
ρ = density (g cm^{-3})

The gas properties γ, κ, η, Cp, and ρ were taken from Ref.(10) at selected values of temperature and pressure and are determined at each experimental temperature and pressure by means of a curve fitting scheme. The wall loss is then calculated for each frequency for comparison with the measured background absorption.

The apparatus losses are associated with the coupling of the acoustic motion of the gas with a relief valve and an isolation valve connected to the tube. It has also been discovered that acoustical pressure fluctuations at the end plates excite the tube shell into longitudinal motion and dissipate a substantial amount of sound energy within the tube structure according to the following selection rule (Ref.4). An odd gas mode can only excite an even shell mode, and an even gas mode can only excite an odd shell mode.

Because of these apparatus losses, there are some frequencies for which the deviation between the theoretical background loss (calculated by the Kirchhoff formula) and the measured background loss exceed 10%. Since the height of the vibrational relaxation peak turns out to be about 8% of the total damping (at room temperature) and with a typical uncertainty in the background damping of about 3%, we can expect a large error in the determination of the relaxation peak. In an effort to reduce the data scatter due to background losses, a differential technique for data evaluation is employed. This method is developed in

Ref.(3). The background data is taken at the same temperature, pressure, and frequency as the test data. Nitrogen is used for background for (f/P) values above 3 Hz/atm and nitrogen with 1% carbon dioxide added is used as background for (f/P) values below 3 Hz/atm. In an effort to reduce the random error in the data, more data points (70-90) were taken to determine $(f/P)_{max}$ than in the previous study with this apparatus (Ref.2). Frequencies in which the deviation between the theoretical background (computed by the Kirchhoff Formula) and the measured background loss exceed 10% were discarded.

IV. DATA EVALUATION AND RESULTS

The acoustic pressure wave acts as a perturbation adding additional translational energy to the molecules of the gas. Through collisions this additional energy is distributed to the vibrational modes of the molecule according to the Equipartition Theorem. Accordingly, (Refs.5-9) the theoretical curve for a two level single relaxation process is given by:.

$$\mu = Z\,\mu_{max}\,\frac{(f/P)\cdot(f/P)_{max}}{(f/P)^2 + (f/P)^2_{max}} \qquad (3)$$

where for diatomic molecules

$$\mu_{max} = \frac{2\pi}{35}\,(1-h)\left\{\frac{\Theta}{T}\right\}^2\,\frac{\exp(-\Theta/T)}{(1-\exp(-\Theta/T))^2} \qquad (4)$$

Here $(f/P)_{max}$ is the location on the frequency/pressure axis of maximum absorption , due to vibrational relaxation, (Hz/atm) and μ is the sound attenuation (neper/wavelength). The parameter h is the fractional molar concentration of water vapor and Θ is the characteristic vibration temperature (3352 Kelvin for nitrogen). Eq.(3) is known as the Debye Relaxation Equation and Eq.(4) is based on the Planck-Einstein Formula

for specific heats. The relaxation time is known to be the inverse of $2\pi f_{max}$. The relation between the relaxation time and the transition probability (k) for deexcitation per molecule per second is found from the rate equation for a two level single relaxation process and is given by:

$$1/\tau = k_{10} \{1 - \exp(-\theta/T)\} \quad (5)$$

The collision number is the ratio of the relaxation time to the mean free time between collisions. The mean free time is known from Kinetic Gas Theory and is given by:

$$\bar{\tau} = \frac{1}{4Na\ P\ D^2}\left\{\frac{M\ k\ T}{\pi}\right\}^{1/2} \quad (6)$$

where

Na = Avagadro's Number
P = pressure (Nt/m^2)
D = molecular diameter (m)
M = molecular weight (kg/mole)
k = Boltzman's constant
T = temperature ^{o}K

Since the mean free time is inversely proportional to the pressure, (f/P) is the correct independent parameter rather than frequency.

Table II contains the results of the impurity analysis (by gas chromotography) of the nitrogen used in this study. A dew point measurement of the nitrogen revealed a water vapor content of 8.7 parts per million (ppm) at 298 Kelvin. This corresponds to data set number six in Table III. The location of the vibrational relaxation peak of nitrogen is known to shift to higher (f/P) values with increasing humidity (Ref.2). A series of data was taken in eight

TABLE II. NITROGEN IMPURITY ANALYSIS

DATA SET	IMPURITY CONTENT by GAS CHROMOTOGRAPHY (ppm)		WATER VAPOR CONTENT by DEW POINT MEASUREMENT (ppm)
	CO_2	O_2	
6	<0.1	<2.	8.7
8	<0.1	<9.	11.1

different sets of nitrogen-water gas mixtures at three different temperatures. The measurements become more difficult and show more scatter at the higher humidities because the higher water vapor concentrations are obtainable only at low nitrogen pressures. The low pressure causes a low acoustical excitation and diminished signal-to-noise ratio, as expanded upon in Ref.(3).

Fig.(1) shows the results of sound absorption measurements in a representative nitrogen-water gas mixture at three different temperatures. Appendix C contains the remainder of the sound absorption measurements of the nitrogen-water gas mixtures made in this investigation. The number under each curve references the data set number in Table III. The vibrational relaxation peak, $(f/P)_{max}$, is determined by an unweighted least squares best fit of the data with the Debye theoretical Relaxation Equation and is the solid line. The peak location along the (f/P) axis is the only adjustable parameter. The peak height is calculated from Eq.(4) and the data is evaluated by the differential technique previously mentioned. The measurements are more difficult and show increased scatter at the low temperature because of the smaller peak height. A compilation of $(f/P)_{max}$ versus humidity appears in Table III and is graphically depicted in Fig.(2) for all three temperatures. The bounds on $(f/P)_{max}$ are 95% confidence intervals based on the F distribution, as discussed in Appendix B. The best fit linear relationship reported by

Figure 1. Representative Sound Absorption Measurements in N_2-H_2O Gas Mixtures

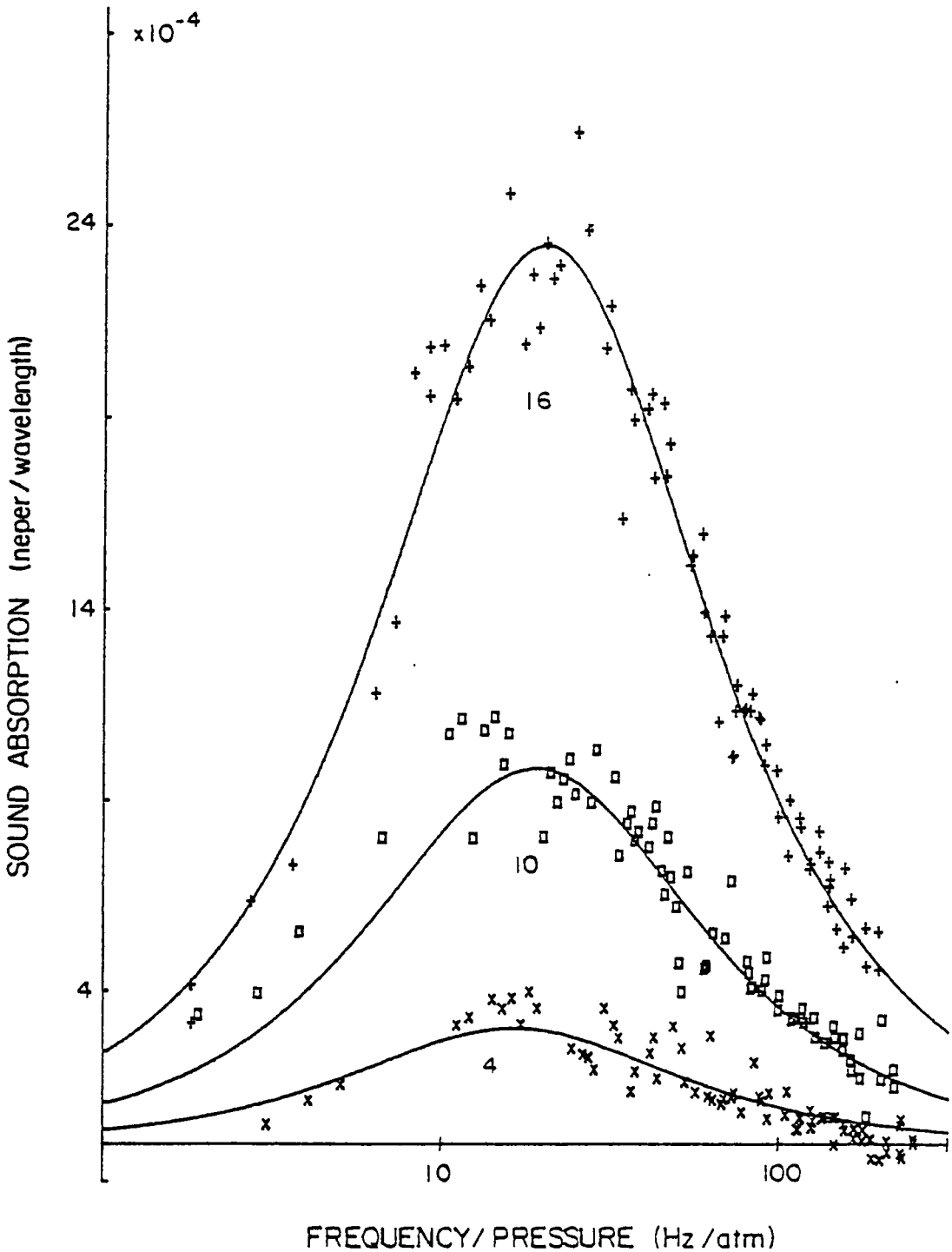

TABLE III. $(f/P)_{max}$ vs Humidity Measurements at Elevated Temperatures

DATA SET	TEMP (Kelvin)	TOTAL PRESSURE (atm)	HUMIDITY (ppm)	$(f/P)_{max}$ (Hz/atm)	BOUNDS on@ $(f/P)_{max}$ (Hz/atm)
1	299	9.31	2023.	36.4	33.1 - 40.0
2	298	4.95	7550.	119.	109 - 129
3	303	9.66	3388.	52.1	48.7 - 55.4
4	299	9.57	915.6	16.2	14.5 - 18.0
5	299	9.33	406.1	9.01	7.77 - 10.4
6	298	80.8;34.3@@	8.7	.167	.139 - .196
19	299	1.00	18480.	385.	340 - 432
20	302	1.02	17790.	352.	320 - 432
7	343	10.5	1980.	39.7	36.4 - 43.1
8	342	5.66	7799.0	133.	124 - 141
9	344	11.0	3422.	61.7	59.4 - 64.3
10	344	11.0	1099.	18.8	17.3 - 19.6
11	344	10.7	432.6	9.43	8.82 - 9.93
12	343	43.5	14.8	.255	.220 - .283
21	343	1.17	21370.	485.	454 - 516
22	342	1.16	28100.	654.	611 - 703
13	387	11.6	2041.	42.0	39.6 - 44.7
14	388	6.30	8050.	136.	129 - 142
15	388	12.3	3609.	64.1	62.2 - 66.1
16	388	12.2	1122.	19.8	19.3 - 20.5
17	388	12.0	538.8	10.5	9.96 - 10.9
18	386	103;58.6@@	11.1	.214	.202 - .225
23	387	1.22	22890.	645.	603 - 672
24	387	1.27	30910.	855.	799 - 909

@ represents a 95% confidence interval based on the F distribution (Appendix B).

@@ Measurements at two pressures were combined into one data set.

Figure 2. Vibrational Relaxation in Nitrogen

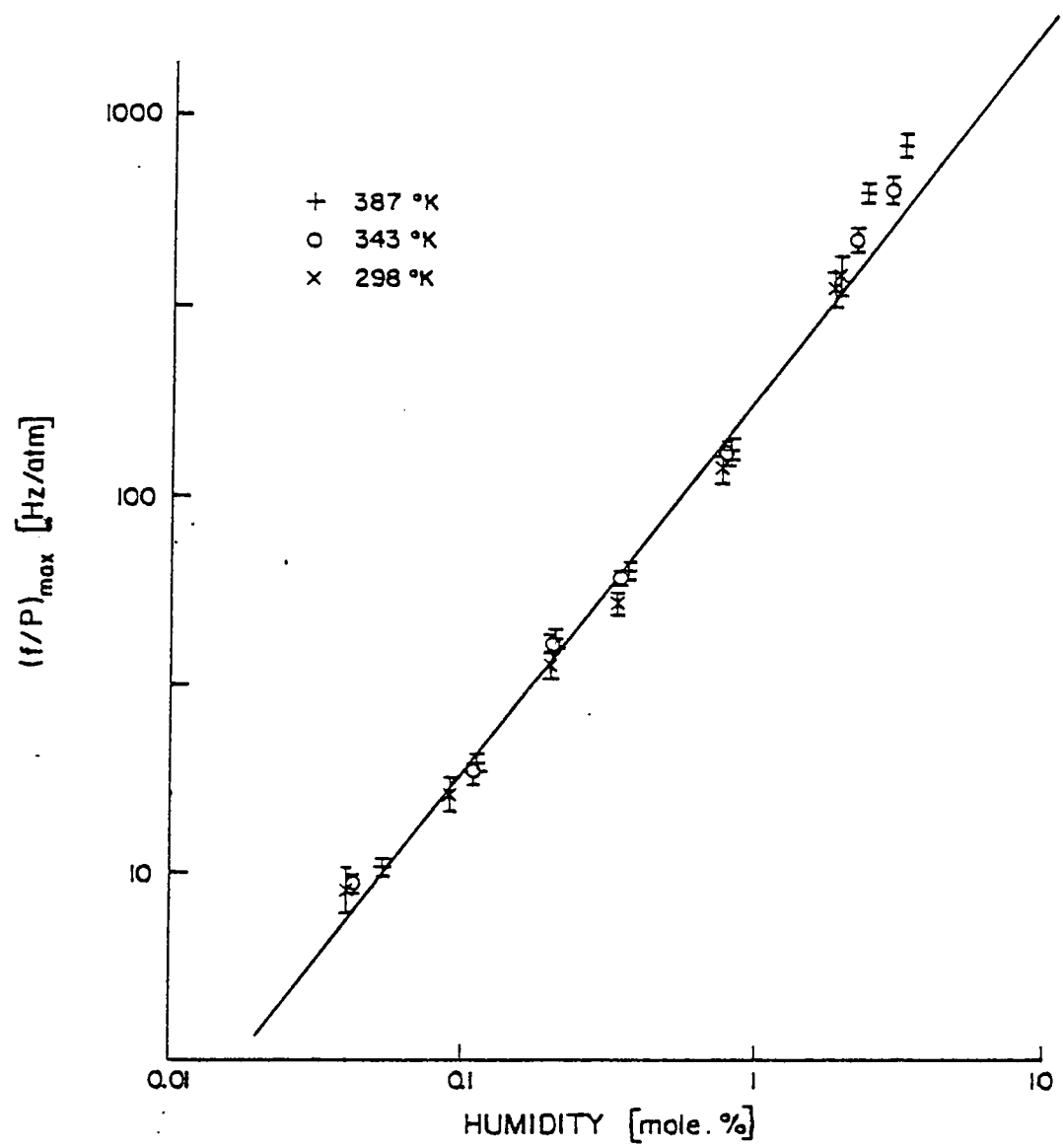

Zuckerwar and Griffin, is shown as the solid line and is given by:

$$(f/P)_{max} = a0 + a1\ h \qquad (7)$$

where $a0 = 0.013 \pm 0.012$ Hz/atm
$a1 = 0.0200 \pm 0.0024$ Hz/atm ppm

This is not a best fit of the data reported here which gives the value of a1 as 0.0184 Hz/atm ppm. At the lower humidity values, the data, within experimental error, show excellent agreement with their relationship. Within the uncertainties of this experiment, no significant temperature dependence was observed in the slope, $(f/P)_{max}/h$, at low humidities.

At the highest humidities (20,000 - 30,000 ppm) of the data reported here, the slope exhibits some form of temperature dependence well beyond the uncertainties of the experiment. Previous measurements by Chang, Shields, and Bass (Ref.12) at higher humidity values, (40,000 - 186,000 ppm) were interpreted as showing no significant temperature variation in the slope in the temperature range 311-415 Kelvin. They report the following relation:

$$(f/P)_{max} = a1\ h \qquad (8)$$

where $a1 = 0.260$ Hz/atm ppm

This slope is significantly higher than that reported in 1979 by Zuckerwar and Griffin and obtained in this work.

In an effort to consolidate low and high humidity data, Zuckerwar and Griffin proposed an energy transfer

model where the vibration-vibration transfer (V-V) provides the dominant relaxation path rather than the vibration-translation transfer (V-T) previously favored for deexcitation of nitrogen by water (Ref.12). The V-V model is based on the following set of energy transfer reactions (Ref.13 and Ref.14):

$$N_2^* + N_2 \leftrightarrow N_2 + N_2 \qquad (k_{10}, k_{01}) \qquad (9)$$

$$N_2^* + H_2O \leftrightarrow N_2 + H_2O \qquad (k_{20}, k_{02}) \qquad (10)$$

$$N_2^* + H_2O \leftrightarrow N_2 + H_2O^* \qquad (k_{30}, k_{03}) \qquad (11)$$

$$H_2O^* + H_2O \leftrightarrow H_2O + H_2O \qquad (k_{40}, k_{04}) \qquad (12)$$

$$H_2O^* + N_2 \leftrightarrow H_2O + N_2 \qquad (k_{50}, k_{05}) \qquad (13)$$

where the k's are the forward and backward reaction rates. Following a Tuesday-Boudart analysis (Ref.2 and Ref.13) they obtained the following relation for the slope S(h).

$$S(h) = \frac{\{2\pi\ (f/P)_{max} - k_{10}\}}{h} = k_{20} - k_{10} + \frac{k_{30}k_{50} + k_{30}(k_{40} - k_{50})h}{k_{03} + k_{50} + (k_{40} - k_{50} - k_{03})h} \qquad (14)$$

For small humidities, this reduces to:

$$S(h) \rightarrow S1 = \frac{k_{30}\ k_{50}}{Ek_{30} + k_{50}} \qquad (15)$$

where $E = \exp(-\Delta\theta/T)$ and $\Delta\theta$ (1058 °K) is the difference between characteristic temperatures of the vibration modes of nitrogen and water vapor. For large humidities, the deexcitation of water by itself is known to be rapid

($k_{40} >>> k_{30}, k_{50}$) and Eq.(14) reduces to:

$$S(h) \rightarrow S2 \simeq k_{30} \qquad (16)$$

Physically, the deexcitation of nitrogen in water vapor mixtures proceeds by way of reactions (11) and (13) in series at low humidities and by way of (11) and (12) in series at high humidities. Due to the small peak height at 297 Kelvin the scatter in their data is such that the deviation of S(h) from a linear relationship is masked by the uncertainty limits of the data.

Fig.(3) is a plot of S(h) vs the base 10 logarithm of humidity at the three temperatures of this study. The highest humidity data at elevated temperatures, (shown as triangles), are taken from Ref.(12). The solid line is the best fit of Eq.(14) to the data with k_{40} the only adjustable parameter. The data show that the slope, S(h), does exhibit a temperature dependence, in that, as the temperature increases the separation between the low humidity slope, S1, and the high humidity slope, S2, also increases. At the highest two temperatures (343 and 387 Kelvin) the two slopes are separated beyond the error ranges of the data. The two slopes of the low temperature data are masked by the uncertainty of the data.

A Landau-Teller plot of the average of this and previous data below 700 Kelvin, at each temperature, is shown in Fig.(4). Two slopes are clearly evident, the low humidity slope, S1, which is temperature independent (horizontal line) and the higher humidity slope, S2, which

Figure 3. V-V Model Slope vs Humidity
Best Fit Line Determines k_{40}

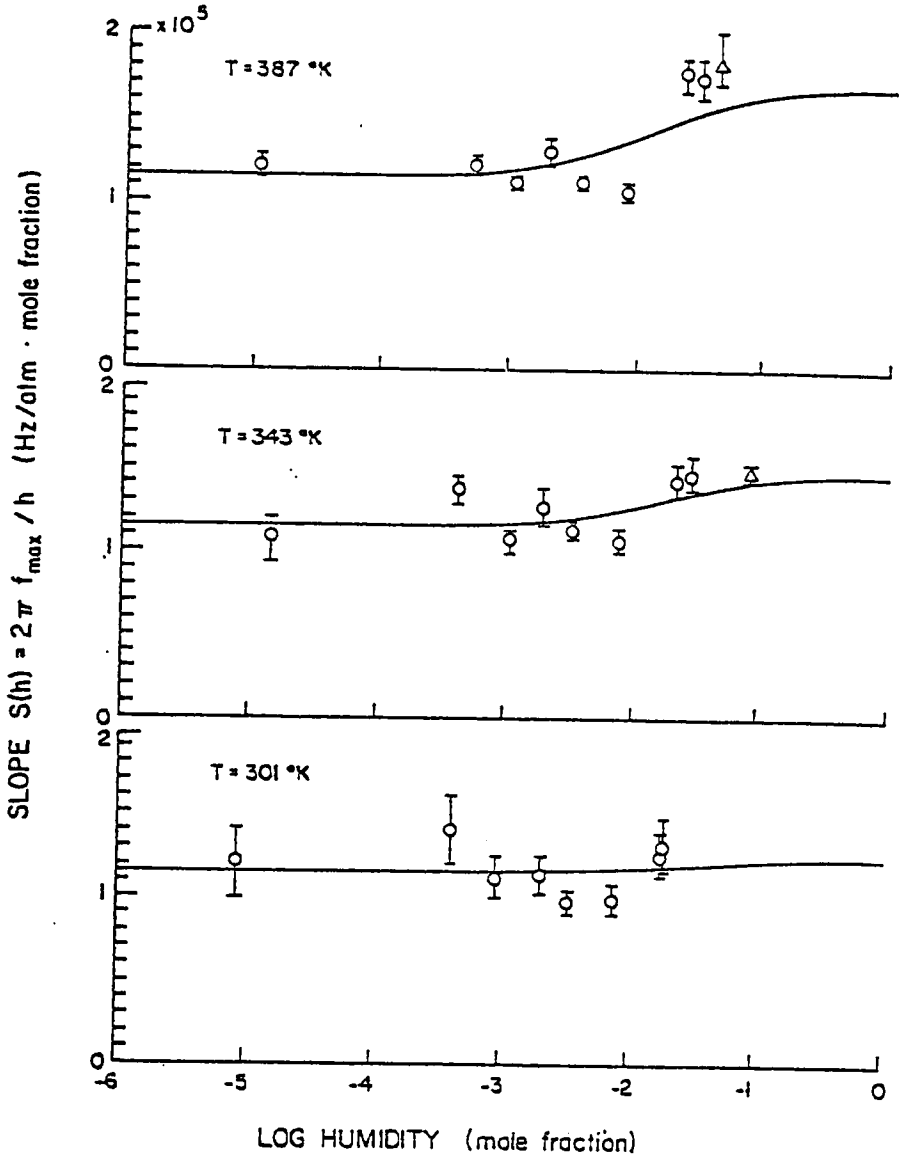

Figure 4. Landau - Teller Plot in 300 - 700 °K Range

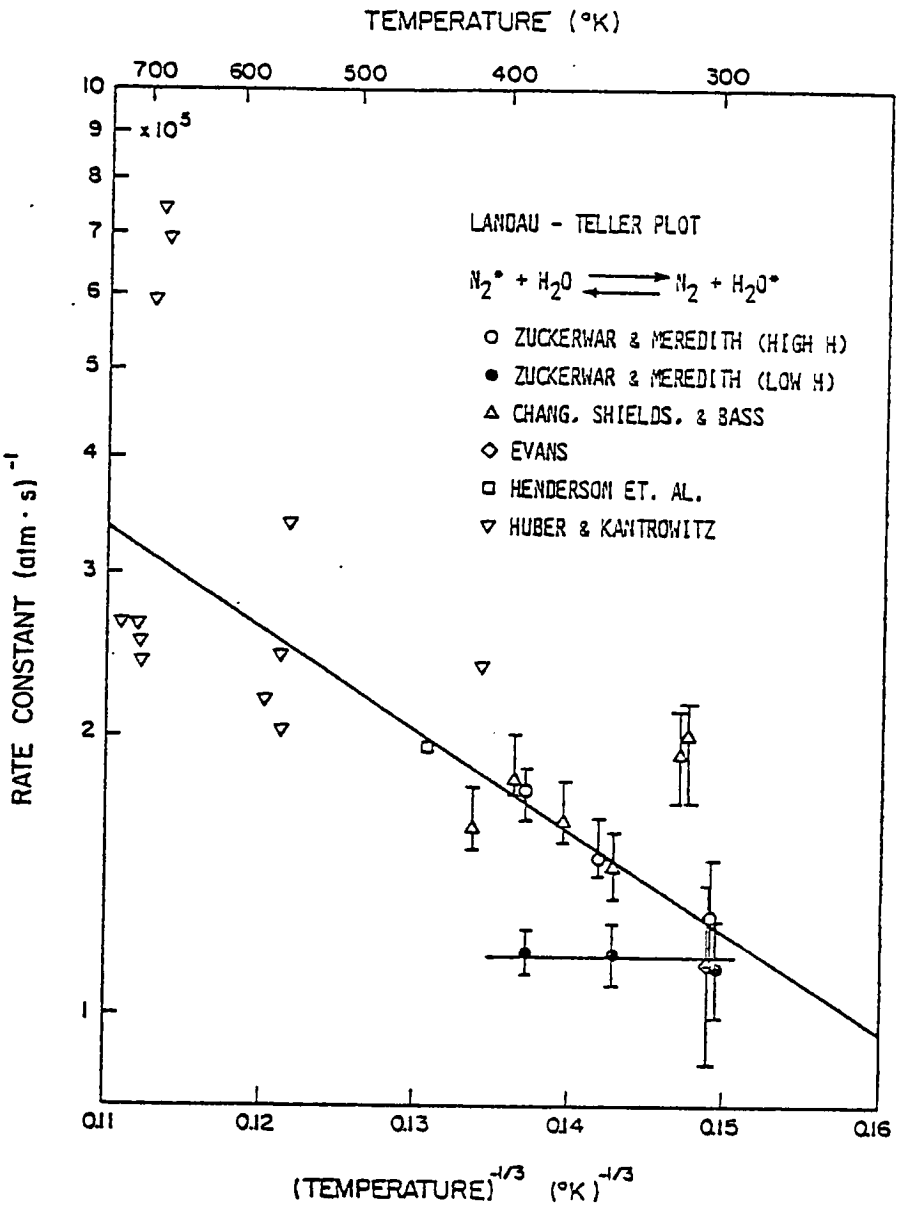

clearly shows the temperature dependence. The solid line is a weighted best fit, excluding the high temperature shock tube data and excluding the highest and two lowest temperature data of Ref.(12). The shock tube data (Ref.17) was excluded because of the large scatter and the other because the rate constant was computed from data only over a small region on the lower flank of the relaxation curve and is thus subject to larger experimental error. The weighting factor was the number of humidity values used in averaging the rate constant at each temperature. Table IV lists the reference and values used in determining the temperature dependence of the high humidity slope, S2.

Fig.(5) gives the temperature dependence of the high humidity slope as:

$$S2 = k_{30} = A \exp[-B/T^{1/3}] \qquad (17)$$

where $A = 5.406 \times 10^{6}$ $(\text{sec atm})^{-1}$

$B = 25.27$ $(^{\circ}K)^{1/3}$ The constants A and B are determined from the data at 342 and 387 Kelvin. Center and Newton (Ref.18) report values:

$A = 3.86 \times 10^{6}$ $(\text{sec atm})^{-1}$

$B = 21$ $(^{\circ}K)^{1/3}$

based on their data in the temperature range 1600-3100 Kelvin. Nagel and Rogovin (Ref.19) report the values:

$A = 2.56 \times 10^{7}$ $(\text{sec atm})^{-1}$

$B = 27$ $(^{\circ}K)^{1/3}$

TABLE IV. LANDAU - TELLER COMPILATION

REFERENCE	TEMPERATURE (Kelvin)	AVERAGE K_{-1} (atm sec)	WEIGHT
This work	301	1.28×10^5	2
	343	1.45	2
	387	1.75	2
Ref.(15)	302	1.13	1
Ref.(12)	350	1.48	1
	367	1.62	3
	394	1.81	1
Ref.(16)	448	1.95	5

determined empirically from their review of data near 1000 Kelvin.

The rate constant, k_{50} , can be determined from Eqs.(15) and (16).

$$k_{50} = (E\ S1\ k_{30})/(k_{30} - S1) \qquad (18)$$

where S1, determined from the slope of the low humidity data in Fig.(2), is found to be 1.16×10^5 $(\text{sec atm})^{-1}$. Assuming the same temperature dependence of the form given in Eq.(17), the values of the constants A and B for the rate constant k_{40} are determined from the best fit of Eq.(14) to the data in Fig(3). Since k_{30} and k_{50} are known, k_{40} is the only adjustable parameter and its constants are found to be:

$$A = 5.76 \times 10^9 \quad (\text{atm sec})^{-1}$$

$$B = 55.1 \quad (^\circ K)^{1/3}$$

V. COMPARISON WITH ANSI STANDARD

Upon substituting the rate constants determined above into Eq.(14), one obtains the following relation between $(f/P)_{max}$ and humidity in air.

$$(f/P)_{max} = \frac{0.781}{2\pi} \frac{k_{30}(k_{50} + k_{40}\, h)}{Ek_{30} + k_{50} + k_{40}\, h} \qquad (19)$$

where

$$k_{30} = 5.41 \times 10^{6} \exp[-25.3/T^{1/3}]$$

$$k_{40} = 5.76 \times 10^{9} \exp[-55.1/T^{1/3}]$$

$$k_{50} = E\, S1\, k_{30} /(k_{30} - S1)$$

$$E = \exp[-1058/T]$$

$$S1 = 1.16 \times 10^{5}$$

all in $(Hz/atm)^{-1}$. The factor 0.781 accounts for the dilution of nitrogen in air. ANSI Standard S1.26/ASA23-1978 gives the following relation for $(f/P)_{max}$ in air:

$$(f/P)_{max} = \left(\frac{T}{273.15}\right)^{-\frac{1}{2}} 3.5 \times 10^{4}\, h \exp(-6.142\, \{(T/273.15)^{-1/3} - 1\}) \qquad (20)$$

The temperature dependence in the standard originates from predictions of the energy transfer theory of Schwartz, Slawsky, and Herzfeld (SSH Theory). The presence of CO_2

in the atmosphere (~ 300 ppm) is known to shift the nitrogen relaxation peak by 3.7 Hz/atm (Ref.8). This effect is excluded in this comparison. The range of the standard, to an accuracy of 10%, is as follows:

Air tempetature 273-313 °K
Relative humidity 10-100%

Table V compares values of $(f/P)_{max}$, in air, computed by both the standard (Eq.20) and the V-V model (Eq.19). As apparent from Table V, the ANSI Standard greatly overestimates the value of $(f/P)_{max}$ as a function of humidity, in the temperature range of the standard.

TABLE V. COMPARISON of VALUES of $(f/P)_{max}$ COMPUTED by V-V Model and ANSI STANDARD

TEMPERATURE (Kelvin)		RELATIVE HUMIDITY 10%	50%	100%
273	V-V	8.65	43.46	87.18
	ANSI	21.11	105.70	211.05
293	V-V	33.03	166.14	334.07
	ANSI	67.12	335.59	671.17
313	V-V	108.17	567.12	1154.44
	ANSI	179.19	895.95	1791.90

VI. CONCLUSIONS

This study presents measurements of acoustical absorption in nitrogen in temperature and humidity ranges previously unobtainable. The vibration-vibration model, proposed by Zuckerwar and Griffin, leads to a theoretical relation, S(h), between $(f/P)_{max}$ and h, which accounts for both the temperature dependence and the transition of the slope, observed in this investigation. The model also synthesizes data obtained at higher temperatures and humidities with that obtained here.

The ANSI Standard evolved from a need for accurate information on sound absorption in air for projects in architectural acoustics, community planning, and noise abatement. Based on this work (and that of Ref.2) the present standard embodies three major shortcomings in predicting the relaxation peak of nitrogen for a given temperature and humidity. The standard predicts an excessively large value for $(f/P)_{max}$, it contains an erroneous temperature dependence, and it does not account for the observed transition between the low and high humidity slopes.

REFERENCES

(1) American National Standard Method for the Calculation of the Absorption of Sound by the Atmosphere, ANSI Standard S1.26/ASA23-1978.

(2) A.J. Zuckerwar and W.A. Griffin, accepted for publication, J. Acoust. Soc. Am. (1981)

(3) A.J. Zuckerwar and W.A. Griffin, J. Acoust. Soc. Am. 68, 218-226 (1980)

(4) A.J. Zuckerwar, J. Acoust. Soc. Am. 65,Suppl. No. 1, S75, (1979)

(5) J.D. Lambert, Vibrational and Rotational Relaxation in Gasses, Claredon Press, Oxford, 1977

(6) K.F. Herzfeld and T.A. Litovitz, Absorption and Dispersion of Ultrasonic Waves, Academic, New York, 1959

(7) R.T. Beyer and S.V. Letcher, Physical Ultrasonics, Academic Press, New York, 1969

(8) H.J. Bauer, Physical Acoustics, (W.F. Mason, ed.), Vol. IIA., Academic Press, New York, 1965

(9) A.J.Matheson, Molecular Acoustics, Wiley-Interscience New York, 1971

(10) Gas Encyclopedia, Elsevier Scientific Publishing Company, Amsterdam , 1976

(11) Handbook of Chemistry and Physics, 45 Ed., The Chemical Rubber Company, 1964

(12) D. Chang, F.D. Shields, and H.E. Bass, J. Acoust. Soc. Am. 62,577-581, 1977

(13) A.J. Zuckerwar and R.W. Meredith, J. Acoust. Soc. AM., Suppl. 1, Vol.68, S107, 1980

(14) W.A. Griffin, PhD Thesis, Old Dominion University, 1980

(15) L.B. Evans, J. Acoust. Soc. Am., 51,409-411, 1972

(16) M.C. Henderson, ET.AL., J. Acoust. Soc. Am., 45, 109-114, 1969

(17) P.W. Huber and A. Kantrowitz, J. Chem. Phys., Vol.15, No.5,275-281, 1947

(18) R.E. Center and J.F. Newton, J. Chem. Phys., 68(8), 3327-3333, 1978

(19) J. Nagel and D. Rogovin, J. Chem. Phys., 72(12), 6593-6601, 1980

APPENDIX A. CAMBRIDGE SYSTEMS DEW POINT HYGROMETER

I. Principles of Operation

The humidity of the test gas was measured using a Cambridge Systems Model 992 Industrial Dew Point Hygrometer. It uses two independent electrical systems in its operation. One is used for automatically and continously controlling the mirror temperature at the dew point and a second, separate system for continously measuring and displaying the temperature of the mirror as it is controlled at the dew point.

A gas sample is directed onto the mirror at a flow rate of two cubic feet per hour. Output from the unbalanced optical bridge controls the cooling current. As the cooling current is increased, the mirror cools and dew accumulates on the mirror. Should the dew layer thicken, the cooling current is decreased (or reversed) until a stable current is attained, whereby a thin film of dew is maintained on the mirror surface. By definition, this represents the dew point temperature.

II. Calibration

Calibration of the Model 992 was done by NASA/LANGLEY against an EG&G Model 136 Hygrometer traceable to the

National Bureau of Standards reference. Calibration data appear in Table AI. Both a quadratic and a linear regression were computed for the calibration data. They are:

$$\text{dew point Celsius} = -75.6902 + 22.4183\ V - 0.4629\ V^2$$
$$\text{dew point Celsius} = -74.3750 + 20.4260\ V$$

where V is the hygrometer output in volts. For dew points within the range of the calibration data, the quadratic form was used to compute the dew point and for dewpoints outside the calibration range, the linear regression was used. Conversions from dew point temperature to water vapor concentration were computed from existing tables (Ref.11).

The error in the dew point measurement, as stated by the manufacturer is as follows. For dew points between -20 and 200 °F the error is 1.0 °F. This corresponds to 530 ppm for a dew point of 55 °F, or about 3.6% of that measurment. For a dew point of -20 °F this corresponds to 24 ppm or about 5.7%. For dew points less than -20 °F the error increases in a linear fashion to 3.0 °F at a dew point of -100 °F, this corresponds to 0.14 ppm, or about 8.3%.

TABLE A1. DEW POINT HYGROMETER CALIBRATION DATA

STANDARD DEWPOINT (Celsius)	HYGROMETER OUTPUT VOLTS
-70.6	0.25
-60.0	0.68
-40.3	1.64
-23.0	2.46
-16.1	2.84
- 3.0	3.51
10.0	4.17

APPENDIX B. LEAST SQUARES FIT TO THE DEBYE THEORETICAL VIBRATIONAL RELAXATION CURVE

A least squares procedure is used to fit the Debye Equation (Eq.3) to the set of measured sound absorption data. To determine the best fit value of $(f/P)_{max}$ it is convenient to use $A = 1/(f/P)_{max}$ as the adjustable parameter. Let $U_i(A)$ be the estimated value of absorption from Eq.(3) and M_i the measured value of absorption. The sum of the squares of the deviations, S(A), is then minimized and thus determines the value of A for the best least squares fit. S(A) is given by:

$$S(A) = \Sigma [\, U_i(A) - M_i \,]^2 \qquad (B.1)$$

This procedure was numerically implemented in BASIC and the calculations done on an HP Model 9830A desk calculator. The first approximate value of A is obtained from the peak location of a graph of that set of data. A is varied by small increments and S(A) recomputed until it reaches a minimum value yielding the best fit.

The bounds on A are determined from the F distribution which is designed to test the equality of two variances for small samples. If S(A) is computed for an arbitrary value of A, the F distribution...

$$S(A) \leq S(A')\left[\, 1 + \left(\frac{P}{N-P}\right) \; F(P,N-P,1-\alpha\,)\right] \qquad (B.2)$$

can be used to approximate the 100(1-α)% confidence interval. Here P is the number of adjustable parameters, one, and N is the number of data points. It is only approximate because the Debye Equation (Eq.3) is nonlinear in $(f/P)_{max}$ for which A' is its least squares estimator. Knowing P, N, and choosing a 95% confidence interval, one can find F from available tables and the entire right hand side of Eq.(B.1) is known. The parameter A is varied until S(A) equals the right hand side of Eq.(B.1). There are two values of A which fulfill this requirement, A+ and A-. The difference, A+ - A- , represents the 95% confidence interval on A. The error bounds in Table III on $(f/P)_{max}$ are defined as:

$$B = [A-]^{-1} - [A+]^{-1} \qquad (B.3)$$

Since S(A) is an asymmetric function of A, the bound is given in the form B. It should be emphasized that these bounds include only the random errors. Systematic errors due to apparatus instabilities, and calibration inaccuracies are estimated to be less than 5%. It is assumed that any other errors are negligible or random. The total error in the measurement of $(f/P)_{max}$ is estimated to be less than 13%.

APPENDIX C. DATA

All of the measurements made in this study are displayed in the graphs on the following pages and in Fig.(2). The number under each curve refers to the data set in Table III, which contains all of the ancillary measurements for that curve.

As mentioned previously, the value of $(f/P)_{max}$ is determined from the best fit, along the (f/P) axis, of the data to the theoretical curve. The peak height is not an adjustable parameter. The highest temperature data tend to show large scatter at the peak height. This scatter is due to the steepness of the free decay angle (above 55 degrees) at the peak and the behavior of the tangent function approaching 90 degrees.

Figure C1. Sound Absorption Measurements

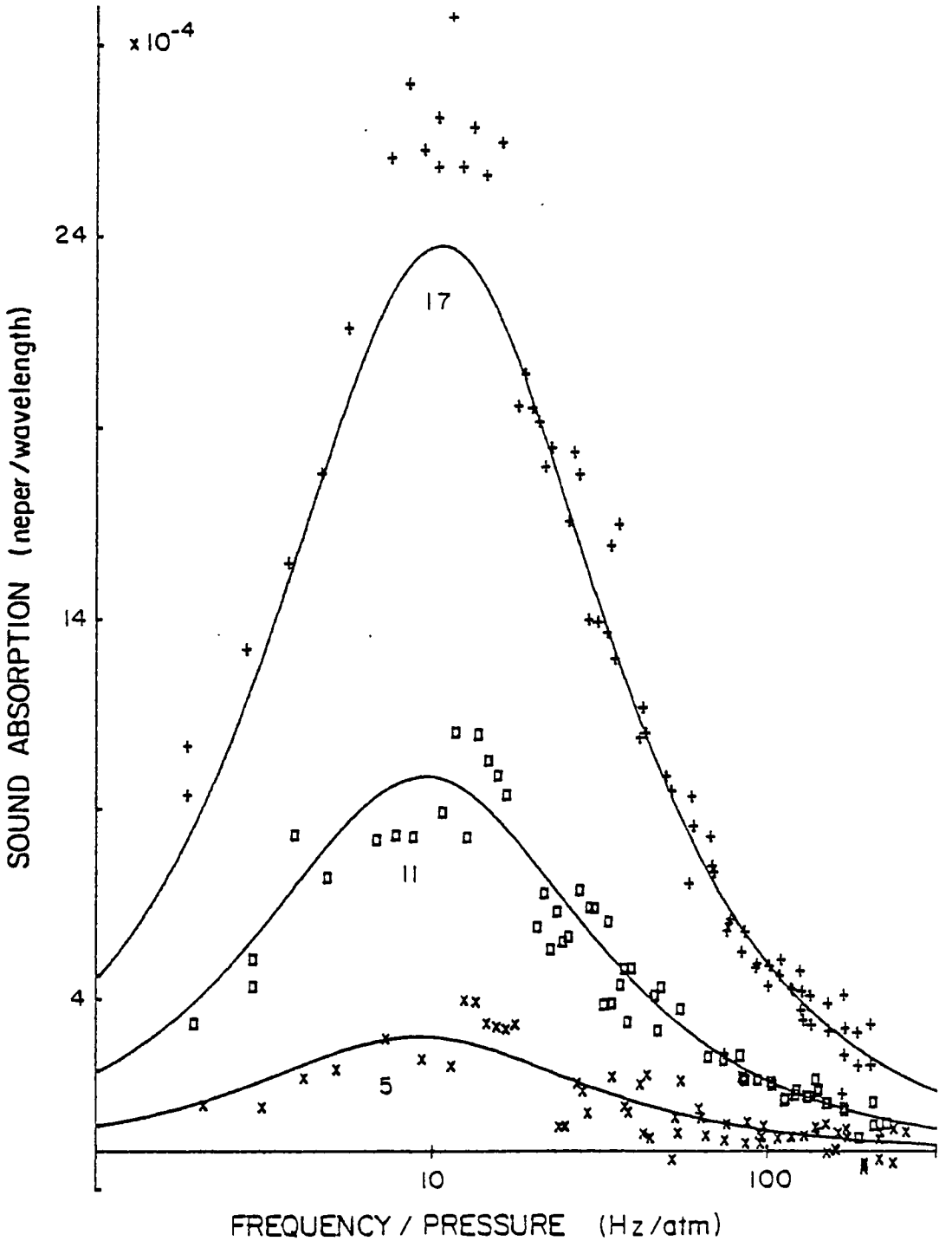

Figure C2. Sound Absorption Measurements

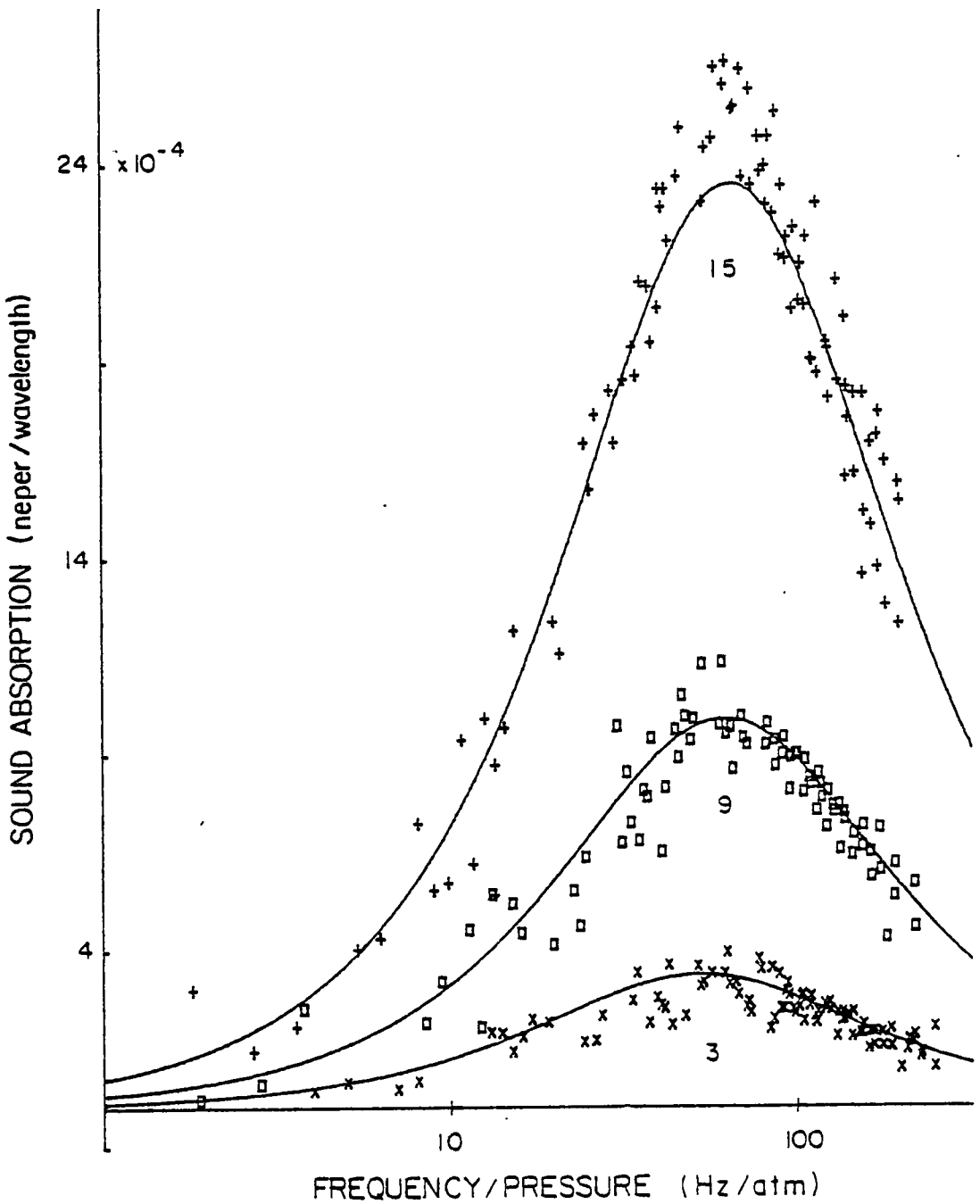

Figure C3. Sound Absorption Measurements

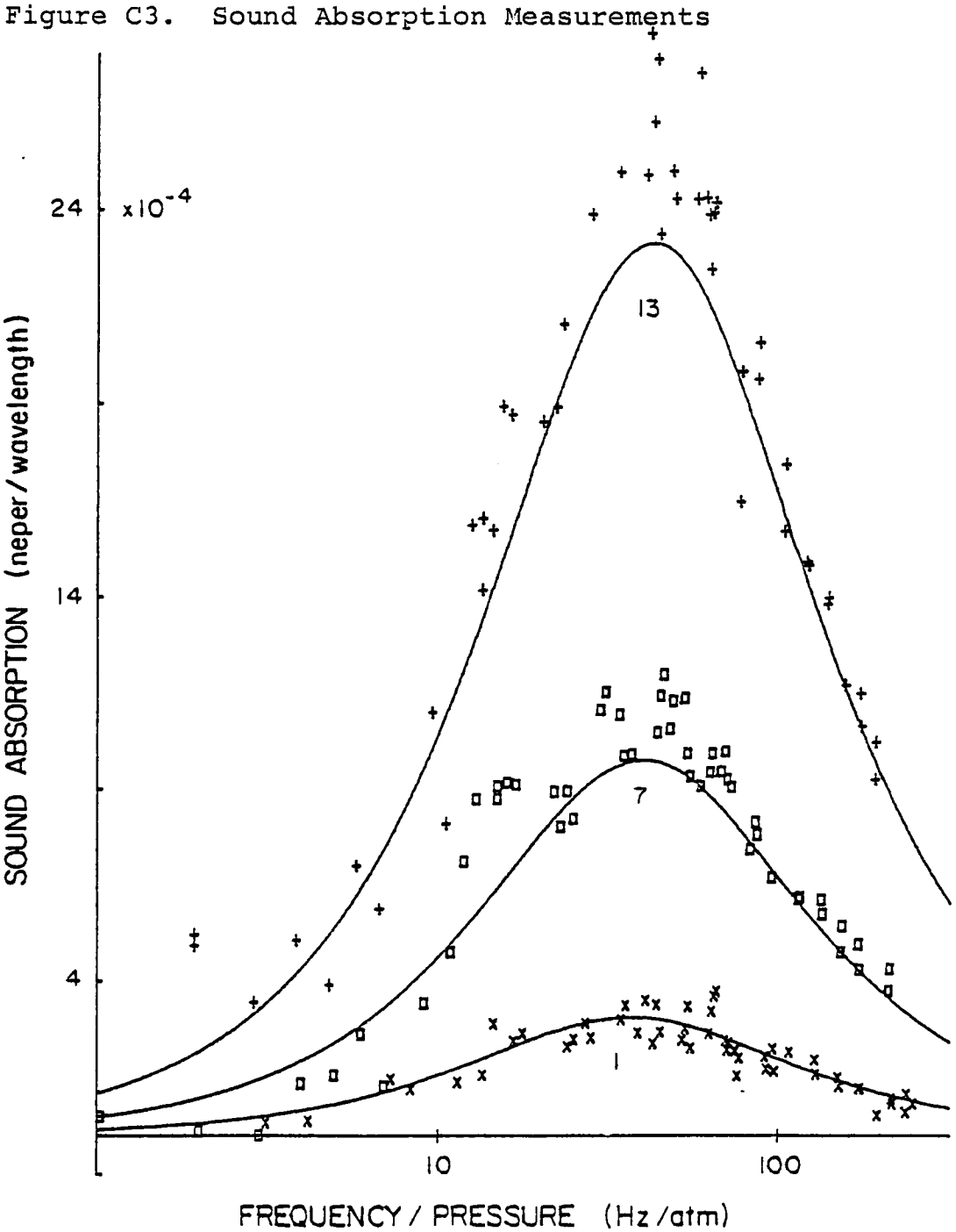

Figure C4. Sound Absorption Measurements

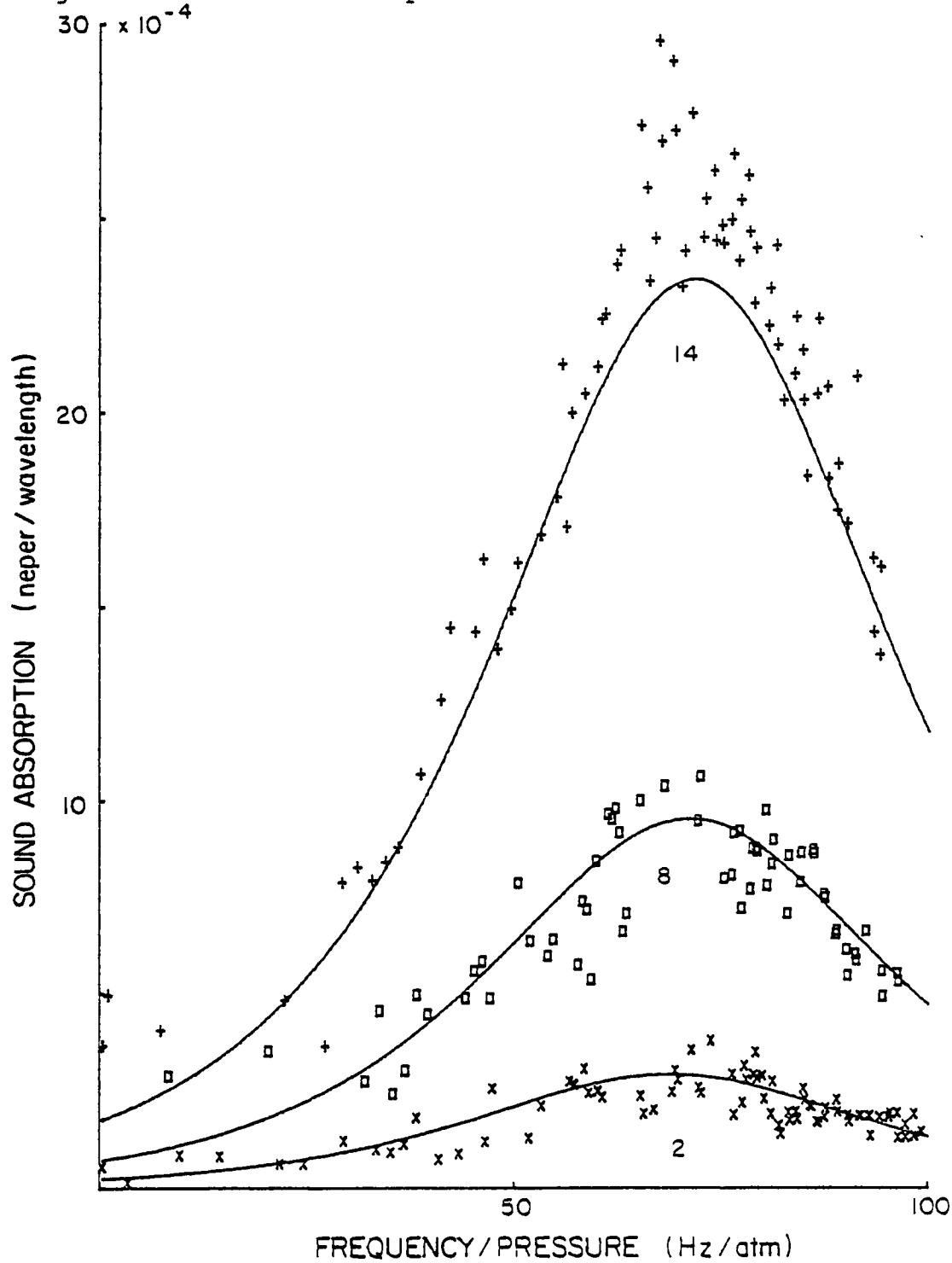

Figure C5. Sound Absorption Measurements

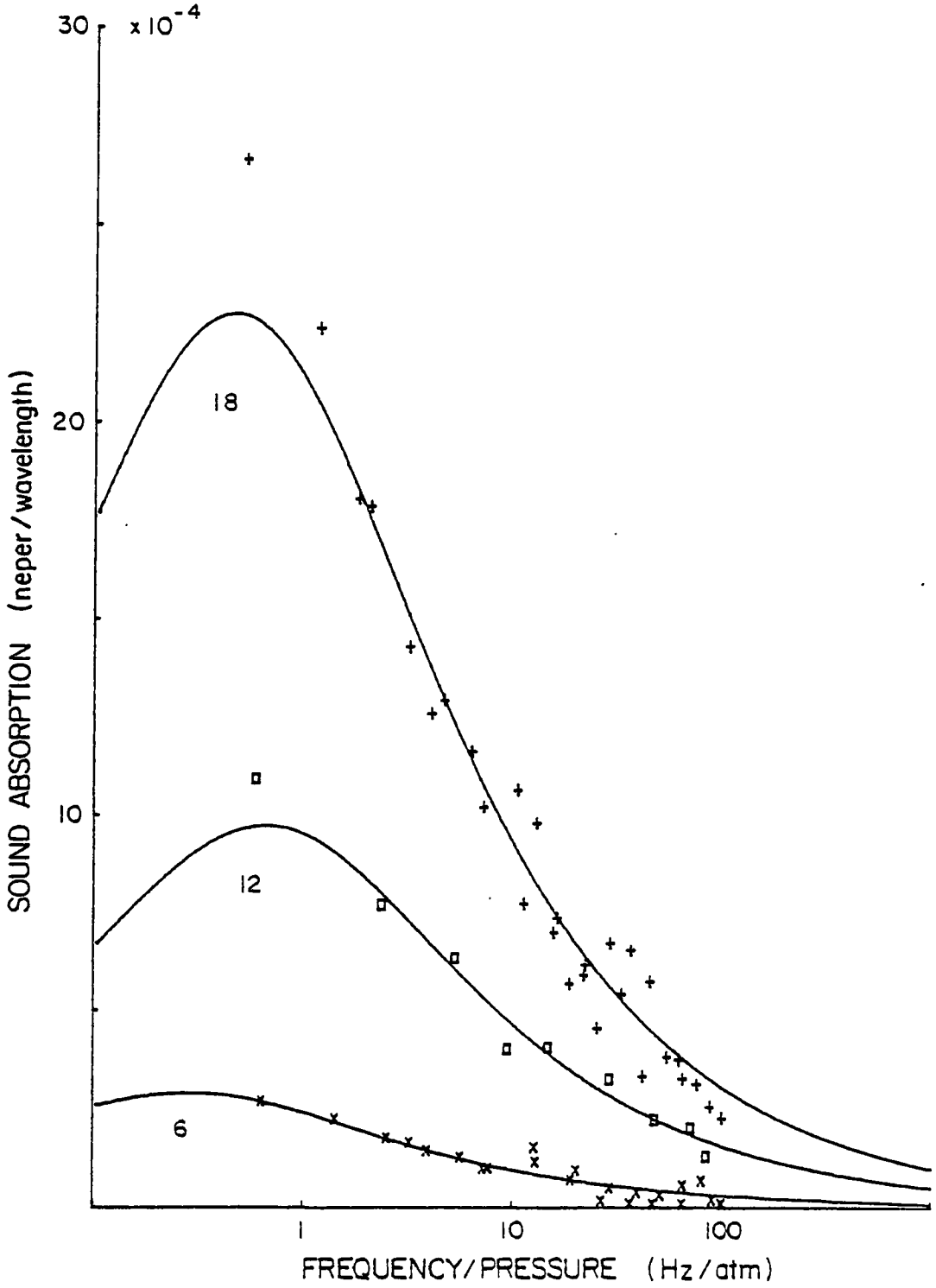

Figure C6. Sound Absorption Measurements

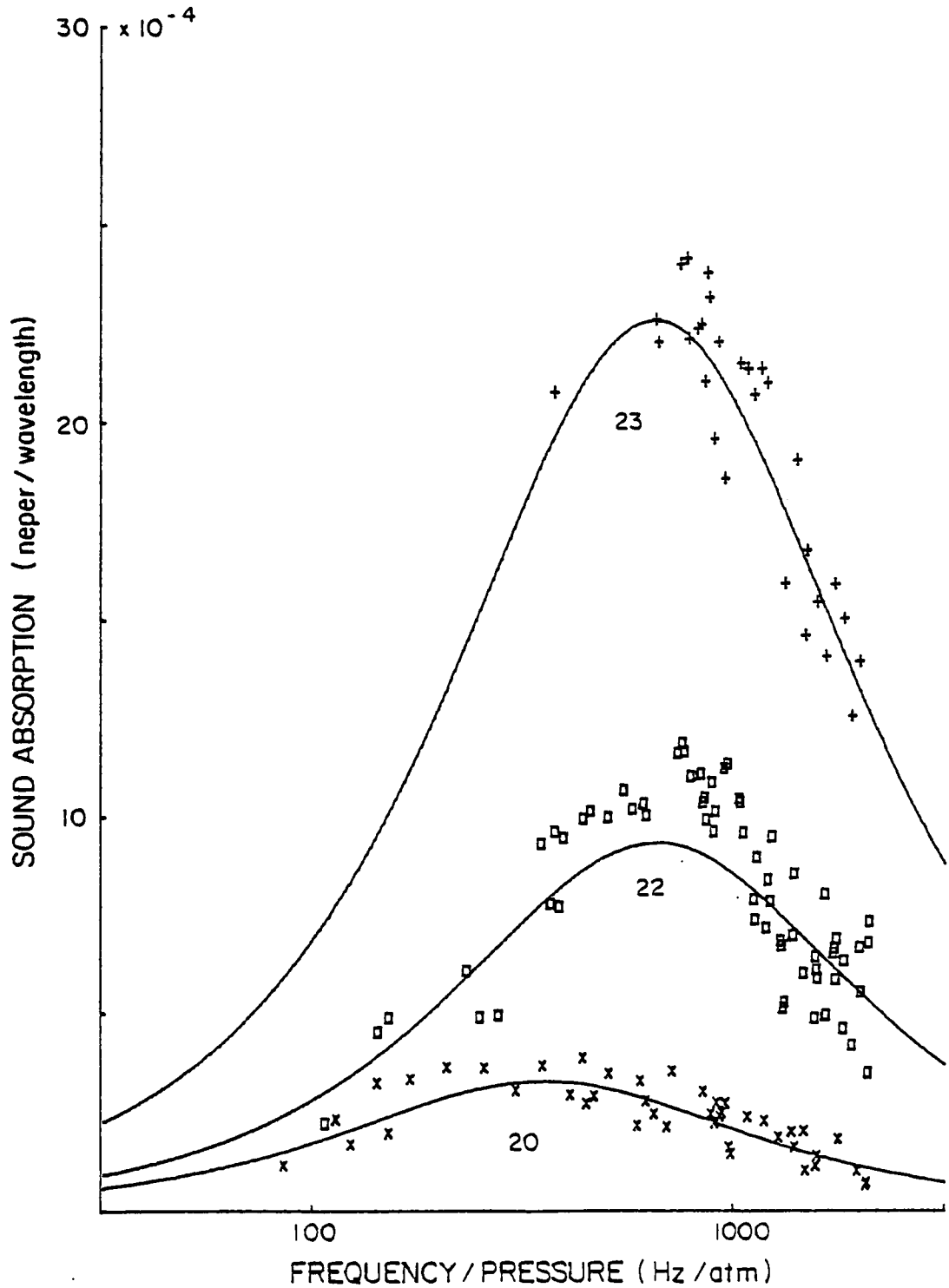

Figure C7. Sound Absorption Measurements